OXFORD

Human Molecular Genetics, 2016, Vol. 25, No. 13 2776–2788

doi: 10.1093/hmg/ddw135
Advance Access Publication Date: 19 May 2016
Original Article

ORIGINAL ARTICLE

Filamin C is a highly dynamic protein associated with fast repair of myofibrillar microdamage

Yvonne Leber[1], Avnika A. Ruparelia[2], Gregor Kirfel[1], Peter F.M. van der Ven[1], Bernd Hoffmann[3], Rudolf Merkel[3,4], Robert J. Bryson-Richardson[2] and Dieter O. Fürst[1,*]

[1]Department of Molecular Cell Biology, Institute for Cell Biology, University of Bonn, D53121 Bonn, Germany, [2]School of Biological Sciences, Monash University, Melbourne, Victoria 3800, Australia, [3]Department of Biomechanics (ICS-7), Institute of Complex Systems, Forschungszentrum Jülich, D52428 Jülich, Germany and [4]Department of Biomechanics, Institute for Physical and Theoretical Chemistry, University of Bonn, D53115 Bonn, Germany

*To whom correspondence should be addressed at: Department of Molecular Cell Biology, Institute for Cell Biology, University of Bonn, Ulrich-Haberland-Str. 61a, D53121 Bonn, Germany. Tel: +49-228-735301; Fax: +49-228-735302; Email: dfuerst@uni-bonn.de

Abstract

Filamin c (FLNc) is a large dimeric actin-binding protein located at premyofibrils, myofibrillar Z-discs and myofibrillar attachment sites of striated muscle cells, where it is involved in mechanical stabilization, mechanosensation and intracellular signaling. Mutations in the gene encoding FLNc give rise to skeletal muscle diseases and cardiomyopathies. Here, we demonstrate by fluorescence recovery after photobleaching that a large fraction of FLNc is highly mobile in cultured neonatal mouse cardiomyocytes and in cardiac and skeletal muscles of live transgenic zebrafish embryos. Analysis of cardiomyocytes from *Xirp1* and *Xirp2* deficient animals indicates that both Xin actin-binding repeat-containing proteins stabilize FLNc selectively in premyofibrils. Using a novel assay to analyze myofibrillar microdamage and subsequent repair in cultured contracting cardiomyocytes by live cell imaging, we demonstrate that repair of damaged myofibrils is achieved within only 4 h, even in the absence of *de novo* protein synthesis. FLNc is immediately recruited to these sarcomeric lesions together with its binding partner aciculin and precedes detectable assembly of filamentous actin and recruitment of other myofibrillar proteins. These data disclose an unprecedented degree of flexibility of the almost crystalline contractile machinery and imply FLNc as a dynamic signaling hub, rather than a primarily structural protein. Our myofibrillar damage/repair model illustrates how (cardio)myocytes are kept functional in their mechanically and metabolically strained environment. Our results help to better understand the pathomechanisms and pathophysiology of early stages of FLNc-related myofibrillar myopathy and skeletal and cardiac diseases preceding pathological protein aggregation.

Introduction

The myofibrillar apparatus of contracting striated muscle cells is constantly under enormous mechanical strain. Particularly increased workload results in the occurrence of microdamage at the level of sarcomeres, raising the need for dedicated mechanisms to repair damaged myofibrils, while the cardiomyocytes retain their capability to contract. The cytoskeleton provides both scaffolding and signaling functions to facilitate and regulate such repair processes. Previous work in skeletal muscle showed that filamin C (FLNc) and its ligands, Xin

Received: February 16, 2016. **Revised:** April 26, 2016. **Accepted:** April 27, 2016

actin-binding repeat-containing proteins (XIRPs) and aciculin, are excellent markers for myofibrillar lesions (1–4).

Filamins (FLNs) are large, homodimeric actin-binding and actin-crosslinking proteins. Their N-terminal actin-binding domain is followed by 24 immunoglobulin- (Ig-) like domains, the last of which is responsible for dimerization of FLNs. Besides filamentous actin, more than 90 proteins including intracellular signaling molecules, receptors, ion channels, transcription factors, and cytoskeletal and cell adhesion proteins have been shown to bind to FLNs (5–7). Accordingly a plethora of functions are attributed to FLNs, including the organization and stabilization of the actin cytoskeleton and its anchorage to transmembrane proteins at sites of cell-substrate- and cell-cell-adhesion (5,6,8,9). Consequently mutations in all three human FLN isoforms, FLNa, FLNb and FLNc, are directly connected to diseases affecting brain, bone, the cardiovascular system and the muscle apparatus (reviewed in 5,10,11).

FLNc is predominantly expressed in skeletal muscles and the heart (12–14), where it localizes to Z-discs, myotendinous junctions, the sarcolemma and intercalated discs (15). It contains a unique insertion of 82 amino acids in Ig-like domain 20 that is not found in the otherwise highly similar FLNa and FLNb. This domain is involved in the interaction of FLNc with several of its muscle-specific ligands. In the Z-disc, FLNc interacts with the calsarcins (FATZ proteins, myozenins) (16–18), myotilin (19) and myopodin (20), while at the sarcolemma FLNc directly binds γ- and δ-sarcoglycans (13) as well as ponsin/CAP (21). Loss of FLNc in mice causes a severe muscle phenotype that includes defects in embryonic myogenesis resulting in a decreased number of primary fibers, excessive fiber size variation, and a disturbance of sarcomere architecture (22). However, loss of FLNc function in zebrafish resulted in myofibril failure consistent with altered sarcomeric architecture, but no effect on myogenesis (23). In humans, FLNc is dramatically redistributed in a large variety of muscle diseases (3,13,24–26). Furthermore, mutations in the gene encoding FLNc (*FLNC*) cause myofibrillar or distal myopathy phenotypes (MFM5, OMIM no. 609524 and MPD4, OMIM no. 614065, respectively) often with cardiac abnormalities (11,27–29). Recently, mutations in *FLNC* were shown to be a novel cause of familial restrictive cardiomyopathy (30) and familial hypertrophic cardiomyopathy (HCM) (31). Unlike cardiomyocytes of HCM patients caused by other mutations, in cardiomyocytes of some of these HCM patients FLNc-containing aggregates were detected. Nevertheless, these patients do not show overt skeletal muscle symptoms of filaminopathy (31).

Recently, both mammalian members of the XIRP family (Xin and XIRP2), were identified as FLNc ligands (32,33). In adult muscle, XIRPs not only colocalize with FLNc at myotendinous junctions of skeletal muscles and intercalated discs of cardiomyocytes but also at sites of small injuries and remodeling (1,34) resulting from exercise and eccentric contractions (4,35,36). In addition to these proteins, myotilin and obscurin have also been reported to be enriched in such areas (35,37,38), implying that the formation and maintenance of myofibrils requires fast and active exchange of proteins between different supramolecular assemblies and cytoplasmic pools. The striking redistribution of FLNc in healthy and diseased skeletal muscle fibers (13,24) also implies that at least some components of myofibrillar Z-discs, i.e. structures that have to withstand considerable forces during muscle contraction and for a long time were supposed to be very stable, are less static than presumed.

To better understand the behavior of FLNc in striated muscle cells, we applied fluorescence recovery after photobleaching (FRAP) to study FLNc dynamics in myofibrillar structures of neonatal mouse cardiomyocytes at different stages of maturation as well as in hearts and skeletal muscle fibers of living zebrafish embryos. Furthermore, we utilized laser-induced microdamage to analyze myofibrillar repair mechanisms in spontaneously contracting cultured mouse cardiomyocytes. Our experiments reveal that FLNc is immediately recruited to areas of myofibrillar damage, repair and remodeling. This feature is enabled by its extraordinarily fast exchange rate and large mobile fraction that were determined by FRAP experiments. In combination with our recent findings of Z-disc instability in filaminopathy patients and filaminopathy knock-in mice (34), our data suggest that FLNc plays an important role in myofibril stabilization and early myofibril repair processes.

Results

FLNc dynamics increases dramatically during myofibril maturation

To analyze FLNc dynamics in living cross-striated muscle cells, we used a previously established cDNA clone encoding FLNc fused N-terminally to enhanced green fluorescent protein (EGFP) (27). Attachment of EGFP to the C-terminus of FLNs was reported not to interfere with dimerization (39) and in transfected muscle cells FLNc-EGFP was mainly targeted to Z-discs and premyofibrils, both locations where endogenous FLNc is also found (15).

To investigate the dynamic behavior of FLNc during myofibril maturation and onset of contractile activity, we transfected mouse cardiomyocytes and subsequently performed FRAP experiments with regions of interest (ROI) comprising either a premyofibril or a single Z-disc of neighboring mature myofibrils. The recovery profiles obtained were in both cases biphasic. Increasing the width of the bleached area resulted in slower increase during the initial recovery but only little variation in the final phase (cf. Supplementary Material, Figure S1). From this we concluded that the initial, fast recovery is at least partially due to lateral diffusion of unbound labeled protein, whereas the later, slower phase indicates the exchange process of bound proteins with the soluble fraction. To account for both phases we used a biexponential fit to determine the halftime of the slower decaying exponential.

$$y\ (t) = \ y_1\left[1 - e^{-K_1 t}\right] + y_2\left[1 - e^{-K_2 t}\right]$$

It should be noted that in FRAP experiments an exponential is only a very rough approximation to the recovery curve calculated for diffusion in homogeneous medium (40,41). Yet, the medium in the close vicinity of a Z-disc or a premyofibril is extremely inhomogeneous and little characterized, therefore only rough estimates of the true recovery curve for molecules diffusing in this complex environment can be given. The fast halftime was typically only few percent (maximum 20%) of the slow halftime, therefore both fit parameters were well separated and had little influence on each other. Thus we believe that in this specific experiment using an exponential to account for diffusion of the unbound molecules is adequate. Moreover, we verified our conclusions by manually determining the halftime. With both methods we reached the same conclusions. The mobile fraction represents a mixture of diffusion and exchange based on binding kinetics. Differences between two groups were assessed by Student's *t*-test. Halftimes, expressed as median ± SD,

mobile fraction as mean ± SD, indicated significant differences of kinetics for these two stages of myofibril assembly.

The exchange of FLNc in mature Z-discs was extremely rapid with a half-life ($t_{1/2\ slow}$) of 18 ± 5 s. 81 ± 8% of FLNc was in the mobile fraction, indicating a very high turnover rate. In contrast, half-lives in non-striated and non-contractile premyofibrils were almost twice as long (34 ± 13 s) and only 63 ± 9% of the protein was mobile (Fig. 1A–D; Supplementary Material, videos1 and 2, Table 1). To compare these results with the dynamics of another Z-disc protein, FRAP experiments were performed on cardiomyocytes transfected with EGFP-tagged α-actinin2, an integral structural component of the Z-disc. Although the mobility

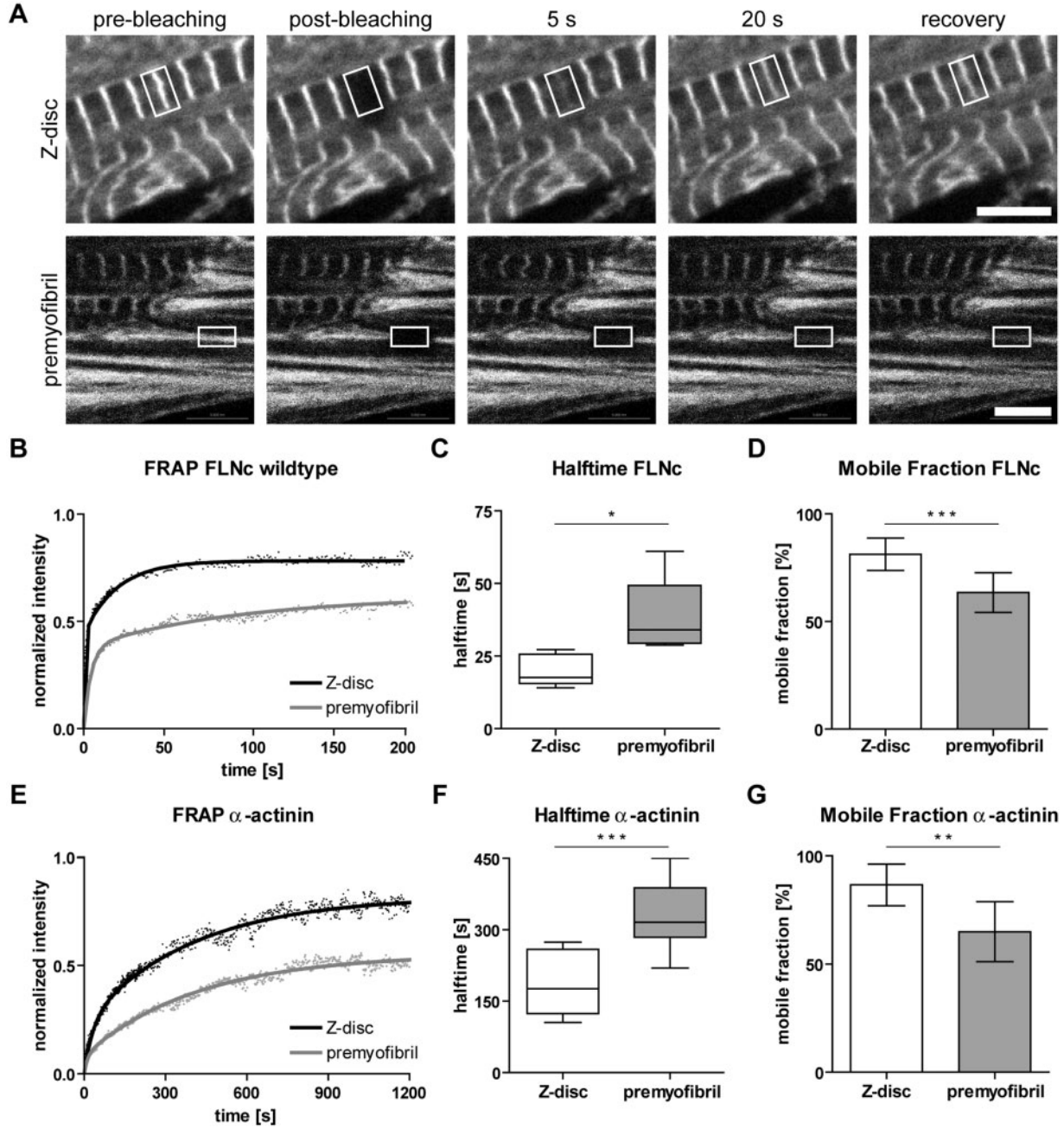

Figure 1. FRAP analysis of dynamics of FLNc and α-actinin in Z-discs and premyofibrils. Neonatal mouse cardiomyocytes were transfected with cDNAs encoding FLNc-EGFP or α-actinin2-EGFP, respectively, and analyzed by FRAP. **(A)** Time series of fluorescence micrographs indicating the localization of FLNc-EGFP in Z-discs (upper panel) or premyofibrils (lower panel), respectively. ROI (indicated by white boxes) were followed over time, and are shown prior to bleaching, immediately subsequent to bleaching and at distinct time points during the fluorescence recovery phase (see also Supplementary Material, video1, Supplementary Material, video2). Bars: 5 μm. **(B)** Typical recovery profile of FLNc in Z-discs and premyofibrils. **(C)** Box plots of halftimes of all experiments show a slow halftime of 18 s (median) in Z-discs and 34 s in premyofibrils, respectively ($n = 8$, shown ± absolute values, $^{*}P < 0.0101$). **(D)** Bar plots summarizing mobile fractions of FLNc in Z-discs and premyofibrils. Note the increase of mobile fraction from 63% in premyofibrils to 81% in mature Z-discs ($n = 8$, shown ± SD, $^{***}P < 0.0005$). **(E)** Typical recovery profile of α-actinin2-EGFP in Z-discs and premyofibrils. **(F)** Box plots of halftimes of all experiments show a slow halftime of 176 s (median) in Z-discs and 316 s in premyofibrils, respectively ($n = 9$, shown ± absolute values, $^{***}P < 0.0004$). **(G)** Bar plot summarizing mobile fractions of α-actinin2 in Z-discs (87%) and premyofibrils (65%), ($n = 9$, shown ± SD, $^{**}P < 0.0011$). Note the considerably higher dynamics of FLNc in comparison to α-actinin2, both in Z-discs and premyofibrils.

of α-actinin2 also increased during myofibril maturation, from 65 ± 14% in premyofibrils to 87 ± 10% in Z-discs, in comparison to FLNc, α-actinin2 recovered significantly slower in both structures with a $t_{1/2}$ of 176 ± 68 s in Z-discs and 316 ± 67 s in premyofibrils, respectively (Fig. 1E–G; Table 1). The comparatively fast recovery rate thus emphasizes the extremely dynamic behavior of FLNc, reinforcing its function mainly in actin-associated signaling rather than being a structural protein.

Table 1. Exchange half-lives ($t_{1/2}$) and mobile fractions (M_f) of transfected EGFP-fusion protein related to region of photobleaching (Z-discs or premyofibrils) and model system (± SD)

Model	Transfected protein	Bleached region	$t_{1/2}$ [s]	M_f [%]
wild-type mouse	FLNc	Z-discs	18 ± 5	81 ± 8
		Premyofibrils	34 ± 13	63 ± 9
wild-type mouse	α-actinin2	Z-discs	176 ± 68	87 ± 10
		Premyofibrils	316 ± 67	65 ± 14
Xin KO mouse	FLNc	Z-discs	14 ± 3	75 ± 7
		Premyofibrils	21 ± 5	63 ± 7
Xin/XIRP2 dKO mouse	FLNc	Z-discs	21 ± 13	84 ± 5
		Premyofibrils	26 ± 12	87 ±18
		cardiac Z-discs	24	95 ± 12
zebrafish	FLNc	skeletal Z-discs	28	99 ± 4
		Myosepta	94	94 ± 9

FLNc dynamics is influenced by specific protein interactions

The striking difference in FLNc dynamics between these two stages of myofibril development implied a distinct regulation of protein interactions. Recently, we showed that both mammalian XIRPs, Xin and XIRP2, simultaneously associate with FLNc via the insertion in its Ig-like domain 20 (32). To investigate the role of these interactions in the differential dynamics of FLNc we analyzed the kinetics of FLNc in cardiomyocytes derived from mice deficient for either Xin alone or both XIRPs. In contrast to wild-type cells, in cardiomyocytes from both genotypes FLNc dynamics in Z-discs and premyofibrils did not significantly differ (Fig. 2B and E, Table 1). This was mainly due to a decrease of the $t_{1/2}$ in premyofibrils from 34 ± 13 s in wild-type cells to 21 ± 5 s in cells lacking Xin (Fig. 2A and B) and 25 ± 12 s in cardiomyocytes deficient for both XIRPs, respectively (Fig. 2D and E). The mobile fraction in premyofibrils was not changed in the absence of Xin alone (63 ± 7%, Fig. 2A and C), but increased from 63 ± 9% (wild type) to 87 ± 18% in cardiomyocytes lacking both Xin and XIRP2 (Fig. 2D and F). Interestingly, dynamics and mobile fractions in premyofibrils lacking both XIRPs resembled those in Z-discs of wild-type cells. These results indicate that the interaction of XIRPs with FLNc plays an important role in stabilizing FLNc specifically in premyofibrils.

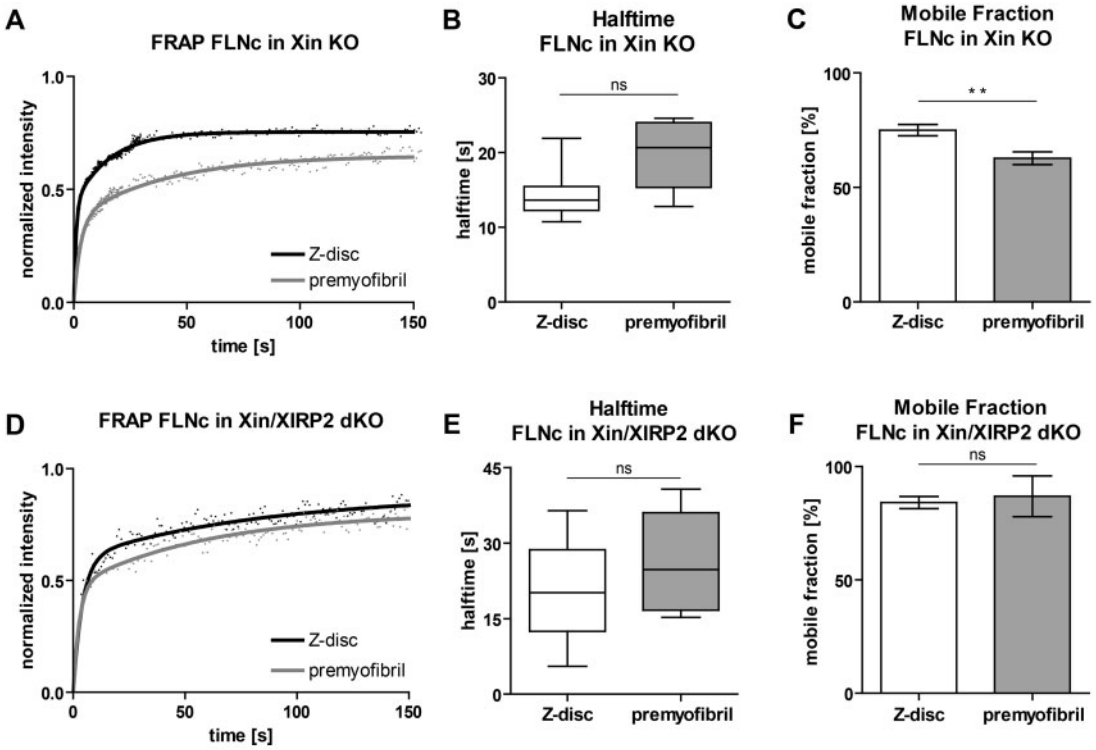

Figure 2. FRAP analysis of FLNc in cardiomyocytes deficient for Xin or both Xin and XIRP2. (**A**) FRAP recovery curves and (**B**) deduced slow halftimes obtained in neonatal mouse cardiomyocytes deficient for Xin and transfected with FLNc-EGFP did not show significantly increased dynamics in premyofibrils or Z-discs when compared with wild-type cardiomyocytes ($n = 7$, shown ± absolute values). Note however, that in contrast to wild-type cells, FLNc dynamics in Z-discs and premyofibrils are not significantly different. (**C**) Mobile fractions in these cells [63% in premyofibrils and 75% in Z-discs ($n = 7$, shown ± SD, $^{**}P < 0.0062$)] were comparable to those in wild-type cells. FRAP experiments in embryonic mouse cardiomyocytes deficient for Xin and XIRP2 transfected with FLNc. **(D, E)** In the absence of both XIRPs, FLNc slow half-lives in mature Z-discs were comparable to those of wild-type cells, whereas also in these cells slow half-lives in premyofibrils were not significantly different from those in Z-discs ($n = 5$, shown ± absolute values). (**F**) The mobile fraction in premyofibrils without XIRPs was significantly increased (87 ± 18%, compared with 63 ± 7% in Xin-deficient and 63 ± 9% in wild-type cells) to values almost identical to Z-disc levels (84 ± 5%, $n = 5$). In contrast, mobility in Z-discs was similar in cardiomyocytes derived from all genotypes.

FLNc is involved in early stages of myofibrillar remodeling and repair

The results described above indicate that FLNc is an extremely dynamic Z-disc protein, and we reasoned that this high exchange rate might be needed to support fast repair and/or remodeling processes. In order to induce localized damage and subsequent repair in a live-cell microscopy setting, we treated FLNc-EGFP-transfected cardiomyocytes with laser pulses at the level of single Z-discs, which resulted in myofibrillar damage and splitting of Z-discs. Z-disc splitting started at the edges of the Z-disc and continued until the complete Z-disc was split. Immediately after damage, FLNc was recruited to the area located between two split Z-discs and thus can be considered as an immediate early marker for damage-induced myofibrillar remodeling processes (Fig. 3).

Subsequently, we studied repair of these lesions in contracting cardiomyocytes that were transfected with both FLNc-EGFP and α-actinin2-RFP. Upon microdamage and splitting of Z-discs, FLNc was again immediately recruited to regions of damage, whereas substantial amounts of α-actinin2 appeared only after 2–10 min, implying distinct contributions of both proteins to myofibril repair processes (Fig. 4A, Supplementary Material, video3). Long-term observations of FLNc and α-actinin2 revealed that sarcomere repair appeared completed three to four hours post damage. Importantly, damaged cardiomyocytes continued to contract during the entire repair process.

In order to investigate whether these repair processes are dependent on *de novo* protein biosynthesis, laser-induced microdamage was performed in the presence of the protein synthesis inhibitor cycloheximide (Fig. 4B). Even in the presence of this drug, in all four analyzed cells repair was completed in the same period of time (between 3 and 5 h), indicating that repair is independent of protein biosynthesis.

Previous studies demonstrated that in injured muscle fibers Xin expression is highly upregulated (3,32,42–45). To better understand the chronological sequence of events in myofibril repair, the involvement of Xin was therefore also investigated. Similar to α-actinin2, Xin (isoform A) was recruited to damaged areas within 2 min. Interestingly, XinA remained strongly enriched in the affected region even after apparent completion of myofibril repair, indicating ongoing regeneration processes up to 6 h after damage infliction (Fig. 4C).

Recently, we also identified aciculin as an FLNc-ligand exhibiting dynamics and mobility properties highly similar to those of FLNc. This prompted us to investigate the recruitment of aciculin to the lesion/repair zones. Indeed, both proteins simultaneously appeared in the damaged areas, reinforcing their tight functional association (Fig. 4D).

The observed recruitment of these actin-binding proteins to myofibrillar repair zones stimulated us to analyze the time course of appearance of actin filaments in lesions by damaging cardiomyocytes expressing Lifeact. Although FLNc was again immediately recruited to the damaged areas, surprisingly, Lifeact-associated actin filaments were not observed in the lesions until approximately 10–20 min after damage infliction. This would indicate that actin is not actively involved in early myofibril repair processes (Fig. 5A, Supplementary Material, video4). This unexpected finding was verified by staining fixed, damaged cardiomyocytes with phalloidin, again showing no reactivity in damage/repair areas for several minutes (Fig. 5B). Furthermore, lack of staining of damaged cardiomyocytes with anti-desmin and anti-tubulin antibodies indicated that neither desmin intermediate filaments (Fig. 5B) nor microtubules (not shown) are involved in early repair processes.

FLNc is also highly dynamic *in vivo* with recovery varying between sites of differing functionality

To investigate the dynamics of FLNc *in vivo* we generated a transgenic zebrafish strain in which human FLNc tagged at its C-terminus with EGFP is expressed under the control of the skeletal muscle α-actin promoter. FLNc-EGFP was mainly targeted to Z-discs, where endogenous FLNc is also primarily localized (Fig. 6A). FRAP experiments were performed on Z-discs of both cardiac and skeletal muscle and at the myosepta at 5 days post-fertilization (Fig. 6B^{i}–D^{iii}). In all three cases recovery was biphasic and FLNc demonstrated different dynamics at each of the three locations (Fig. 6E). FLNc was most dynamic at the cardiac Z-disc with a $t_{1/2}$ of 42 s. In contrast, skeletal muscle Z-discs showed a $t_{1/2}$ value of 54 s and myosepta-localized FLNc had the slowest exchange rate with a halftime of 63 s. A very high percentage of mobile FLNc was evident at all three locations (cardiac Z-disc: 95 ± 8%, $n = 6$; skeletal muscle Z-disc: 94 ± 7%, $n = 5$; skeletal myosepta: 92 ± 6%, $n = 10$, Fig. 6F). The rapid recovery of FLNc at all locations investigated corroborated the highly dynamic nature of this actin binding protein. This is a surprising result because this protein has been thought to be involved in

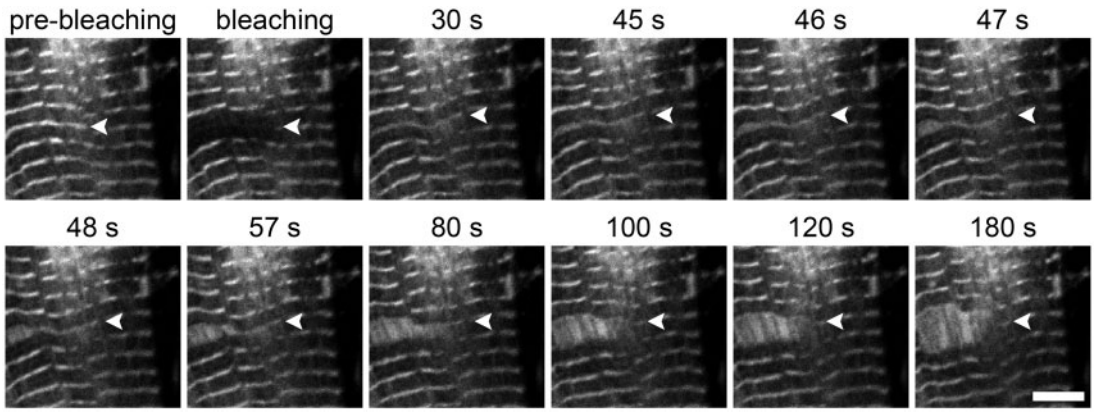

Figure 3. FLNc is involved in early remodeling processes. Laser-induced Z-disc splitting in cardiomyocytes transfected with FLNc-EGFP. Z-disc splitting started 45 s after bleaching at the periphery of the bleached area and continued until the whole Z-disc was split. FLNc was revealed in damage areas in increased amounts relative to normal Z-discs and can therefore be used as a sensitive marker for myofibrillar remodeling. Arrowheads indicate a Z-disc that was split and extended upon bleaching. Bar: 5 μm.

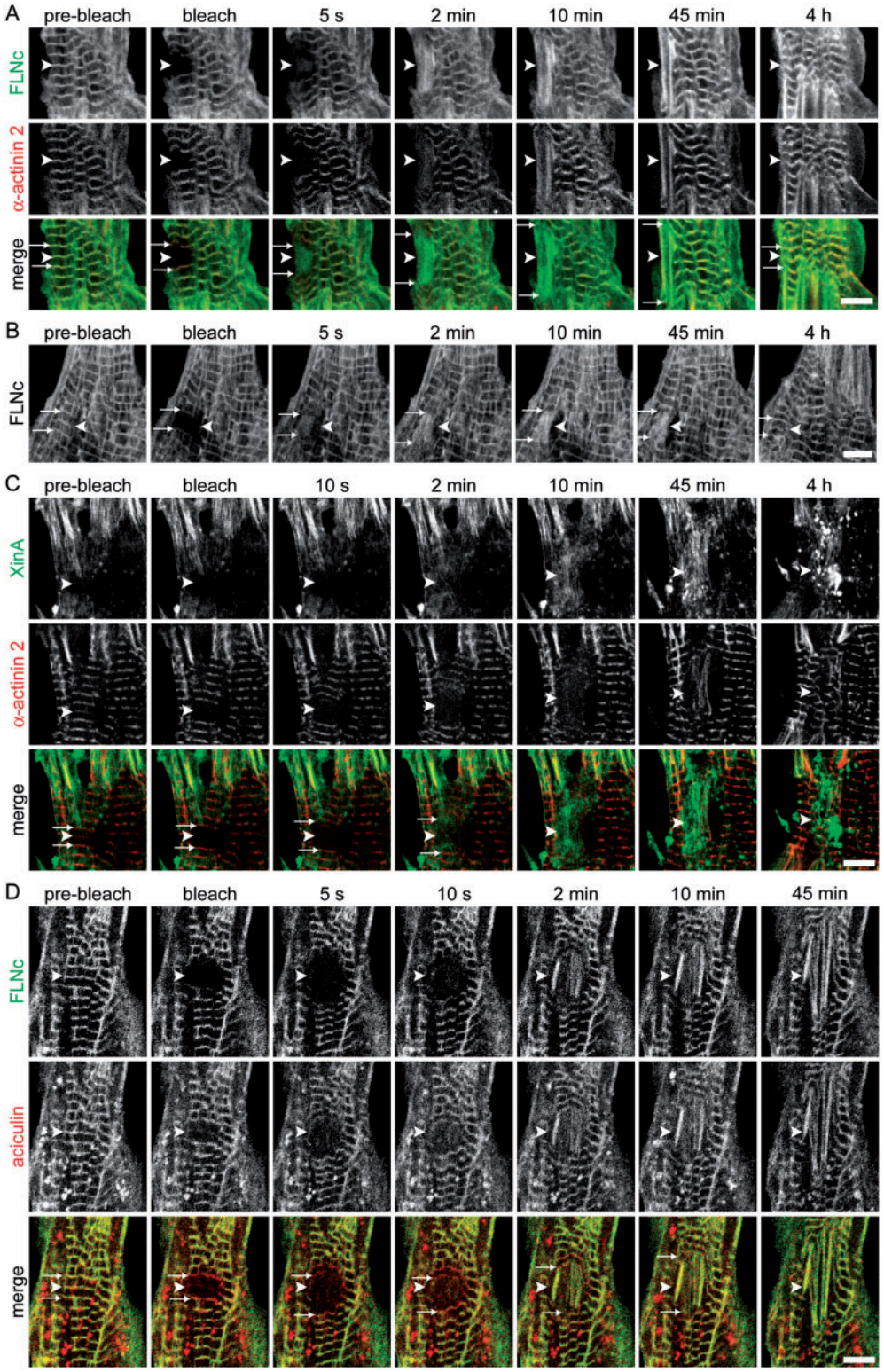

Figure 4. Cytoskeletal proteins are differentially involved in myofibrillar repair. Laser-induced microdamage in cardiomyocytes transfected with either (**A**) FLNc-EGFP and α-actinin2-RFP, (**B**) FLNc-EGFP alone in the presence of cycloheximide, (**C**) XinA-EGFP and α-actinin2-RFP or (**D**) FLNc-EGFP and RFP-aciculin. (A) FLNc was recruited to regions of damage (arrowheads) within seconds, whereas α-actinin2 appeared only after 2–10 min, implying distinct contributions of both proteins to repair processes. After 3–4 h sarcomeres had recovered and myofibrillar repair was completed (Supplementary Material, video3). (B) Inhibition of protein synthesis with cycloheximide does not alter the occurence and time course of myofibril repair in microdamaged cardiomyocytes. Shown is a representative example of four individual experiments. (C) Similar to α-actinin2, XinA was recruited to lesions (arrowheads) after 2–10 min. After four hours XinA was still strongly enriched in the affected region despite apparently complete myofibrillar repair. (D) In contrast to α-actinin2 and XinA, but similar to FLNc, aciculin appeared almost immediately in the damaged areas. In this specific experiment aciculin-RFP was not completely bleached and only seems to appear earlier in the damaged area than FLNc. Arrows mark the unaffected Z-discs flanking the damaged, split Z-discs in (B) and in merged panels of (A,C,D). Bars: 5 μm.

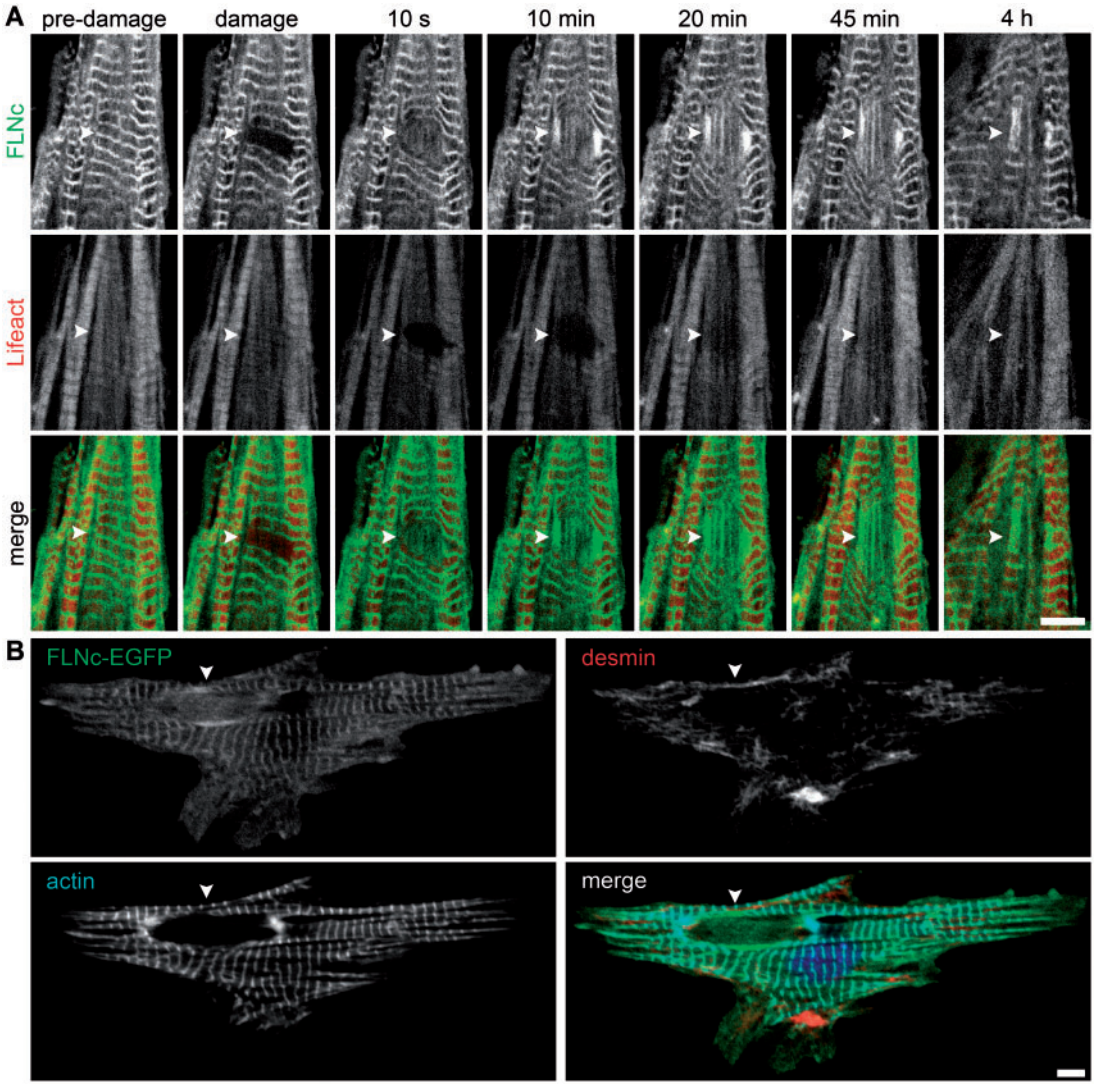

Figure 5. Actin and desmin are not involved in early repair processes. (**A**) Laser-induced microdamage in cardiomyocytes transfected with FLNc-EGFP and Lifeact-Ruby to visualize actin. Although FLNc was immediately recruited to the damaged areas, actin was not found during the earliest stages of myofibrillar repair (10 s, arrowheads) and became detectable only after 10–20 min (Supplementary Material, video4). (**B**) Staining with coumarin-labelled phalloidin and anti-desmin antibody confirmed absence of F-actin and showed the exclusion of desmin intermediate filaments from damaged areas. Cell was fixed 5 min after damage. Bars: 5 μm.

the structural integrity of the Z-disc. Our findings demonstrate that the remarkable mobility of FLNc is preserved amongst vertebrates, irrespective of an *in vitro* cell culture situation or an *in vivo* animal model.

Discussion

The actin-binding and cross-linking protein FLNc is among the first proteins specifically expressed upon the differentiation of striated muscle (12,15). Its important role in adult striated muscles is highlighted by the fact that mutations in *FLNC* cause skeletal muscle diseases and cardiomyopathies (11,27–31). FLNc is a multi-compartment protein located primarily at premyofibrils and myofibrillar Z-discs, with small amounts associated with the sarcolemma (13). In addition, it is highly concentrated at specialized cytoskeleton-membrane attachment sites such as intercalated discs and myotendinous junctions (15). Accordingly, FLNc can bind a wide range of ligands involved in signaling processes, membrane protein organization and actin cytoskeleton regulation. FLNc was proposed to translocate between these different compartments and found to be concentrated at the sarcolemma specifically in myopathic muscle fibers (13). It is, however, entirely unknown how FLNc localization is regulated, whether the dynamic state of FLNc is distinct in these locations, and which specific protein interactions are involved in its regulation. We addressed these questions by analyzing the dynamics of FLNc in cultured cardiomyocytes using FRAP in conjunction with protein interaction assays.

FLNc is a highly dynamic Z-disc protein whose mobility increases during cardiomyocyte myofibril maturation

Our FRAP analysis in zebrafish and contractile mouse cardiomyocytes has revealed that FLNc is a surprisingly dynamic protein with recovery rates of only seconds and an extremely high mobile fraction. This behavior is in sharp contrast to the Z-disc structural protein α-actinin2, which takes several minutes to recover. For both proteins FRAP recovery rates and dynamic

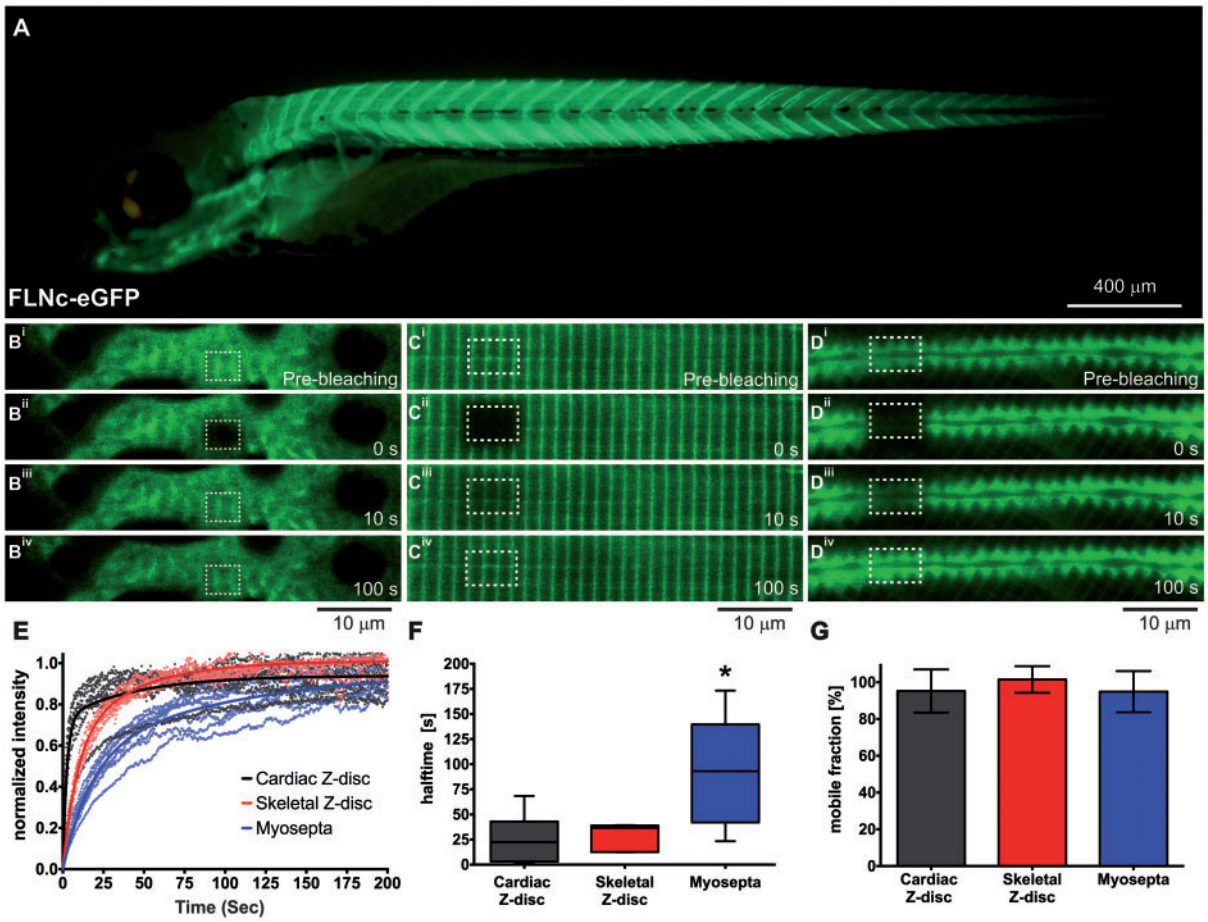

Figure 6. FLNc dynamics in the zebrafish embryo. (**A**) Transgenic zebrafish embryo at 5 days post-fertilization expressing human FLNc tagged to EGFP (FLNc-EGFP) under the *acta1* promoter. Timelapse images documenting fluorescence of FLNc-EGFP before bleaching (pre-bleach), immediately after (0 s), 10 and 100 s after bleaching in (**B**) cardiac muscle. (**C**) Z-discs of the skeletal muscle, and (**D**) in the myosepta of the skeletal muscle. (**E**) Fitted curve of recovery profiles of FLNc-EGFP in cardiac Z-discs (black), skeletal Z-discs (red), and myosepta (blue) shown by solid line. Individual replicates and time points shown in their respective colors (cardiac Z-disc: $n = 6$; skeletal Z-disc: $n = 5$; myosepta: $n = 10$). (**F**) Tukey box plots depicting the median, 25 and 75th percentile, and upper and lower limits of FLNc slow half-lives in cardiac Z-discs (black), skeletal Z-discs (red), and myosepta (blue), with a significantly longer half-life for myosepta localized FLNc (*$P < 0.05$). (**G**) There is no significant difference in the mobile fraction of FLNc between locations (cardiac Z-disc: 95%; skeletal muscle Z-disc: 99%; skeletal myosepta: 94%, shown ± SD).

fractions substantially increased during reorganization of the contractile filaments from premyofibrils to Z-discs. Our experiments show that FLNc is the most dynamic sarcomeric protein described to date, and that other Z-disc proteins, such as α-actinin2, show significantly slower recovery rates. Similar studies in developing myotubes derived from quail skeletal myoblasts demonstrated that the Z-disc proteins myotilin, α-actinin, actinand telethonin, are considerably less dynamic. Furthermore, and in contrast to FLNc, their mobility decreased upon maturation of myofibrils (46–48). These differences, and the divergent dynamics of α-actinin in mouse cardiomyocytes and quail skeletal myotubes ($t_{1/2}$ slow of 176 and 721 s, respectively), most likely result from the application of different striated muscle cell types (cardiomyocytes versus skeletal muscle cells) derived from different species. It is also interesting to note that in quail myotubes telethonin, actin and α-actinin are considerably less dynamic than myotilin, cypher-1s and FATZ (46).

Apparently, myofibrillar Z-discs contain two distinct subsets of proteins: a more static group including α-actinin that mainly fulfils structural functions and a second group of proteins comprising FLNc and aciculin (2) that is less firmly integrated in the core Z-disc structure, but rather involved in signal transduction events and in the ongoing maintenance and repair of the myofibril. Interestingly, an antibody specific for the N-terminus of FLNc localized this part of the protein not to the antiparallel actin filaments within the Z-disc, but rather to its periphery in the area of parallel actin filaments (15). Elucidation of the precise layout of FLNc in the Z-disc region, however, awaits the development of further domain-specific antibodies recognizing different regions of FLNc and their localization at high resolution. In line with the proposed signaling function of FLNc, the Z-disc is increasingly considered to be a nodal point in a signal transduction network involved in mechanotransduction and the control of hypertrophic growth (reviewed in 49). Notably, FLNc has recently been demonstrated to be degraded by chaperone-assisted selective autophagy, which is a tension-induced autophagy pathway essential for mechanotransduction and tissue homeostasis in muscle and immune cells (50,51).

In the zebrafish we observed distinct dynamics of Z-disc localized FLNc, which provides a mechanism for signaling within the sarcomere, compared with myosepta localized FLNc, which is important for the maintenance of structural integrity of the muscle fiber. The differences in FRAP recovery rates for FLNc at the two locations suggests a potential correlation between rate

of exchange and activity of the tissue. Muscle activity will result in increased mechanical and oxidative damage, which consequently necessitates continuous and fast protein exchange to keep the cells functional. The observation that actin dynamics varies depending on the contractile state of cardiomyocytes (52) supports this idea.

Recently analysis of the dynamics of the FLNc variant harboring the first discovered and most prevalent myofibrillar myopathy-associated p.W2710X mutation (28) in zebrafish muscle fibers revealed that the mutation causes decreased dynamics (53). This indicates that this mutation not only causes the protein to aggregate spontaneously (28,44,54), but also reduces the dynamic properties of FLNc.

FLNc mobility is strongly influenced by its binding partners Xin and XIRP2

The striking increase in FLNc dynamics during myofibril maturation, and the transition from a non-contractile to a contractile state, implies the existence of mechanisms regulating its mobility, either by post-translational modifications in response to signaling events or via binding to distinct ligands. An example of the former option is the strong influence of hypertrophy pathways on the dynamics of the thin filament barbed end capping protein capZ in cardiomyocytes (55). Multiple phosphorylation events documented in the literature (56–58) and in databases (e.g. http://www.phosphosite.org; http://www.phosida.com/) indicate that similar mechanisms may also control the dynamics of FLNc. Intriguingly, a comparison of the primary structure of all FLNs highlights the singularity of the insertion-containing Ig-like domain 20 of FLNc, which is involved in multiple protein-protein interactions (19,20,32,33). Interestingly, we previously identified a splice variant of zebrafish FLNc without the insertion in Ig-like domain 20 and showed that this isoform is unable to bind zebrafish Xirp1 (59) leading us to investigate specifically the contribution of the Xin-repeat proteins Xin and XIRP2 to FLNc dynamics. Together with previous biochemical experiments (32) our FRAP analyses in cardiomyocytes deficient for Xin or both XIRPs indeed revealed a major role for these proteins in limiting the exchange and/or mobility of FLNc in premyofibrils, but not in its localization.

FLNc is rapidly recruited to sites of myofibril repair

We have previously demonstrated that FLNc as well as the XIRPs are enriched in regions of myofibrillar remodeling and repair (1,59). In order to examine the dynamics of FLNc recruitment to sites of injury we applied laser-induced microdamage to Z-discs of isolated cardiomyocytes and observed that FLNc was recruited within 10 s to damaged areas. Intriguingly, in these regions FLNc was no longer arranged in a cross-striated pattern at the Z-disc, but was instead continuously distributed along longitudinal strands linking intact Z-discs of remaining, undamaged sarcomeres. Lack of staining with phalloidin and a failure of Lifeact to associate with areas of early repair make it very likely that these stages of the repair process are not apparently dependent on filamentous actin. Likewise, neither intermediate filaments nor microtubules seem to be involved.

Similar results were observed in mechanically stretched rat cardiomyocytes (60). These cells react to the applied strain by addition of sarcomeres and show many disruptions in the regular sarcomeric pattern that are devoid of actin filaments within the first hour after stretching. Only after 2–4 h is accumulation of F-actin observed. These findings confirm our data on the absence of detectable actin filaments in early myofibrillar lesions and suggest the importance of FLNc in preventing collapse of remodeling myofibrils.

Recently, *in vitro* experiments showed that FLNs may act as force sensors and are highly elastic (61,62). Together with our data showing the rapid recruitment of FLNc to sites of injury, this may suggest that FLNc directly provides mechanical support in damaged areas. One single FLNc dimer has a native length of ~200 nm that can be extended several times if the Ig-like domains would unfold. Dimers are able to cross-link even short or mechanically damaged actin filaments, even if they are not detected by standard F-actin localization methods. Several FLNc molecules together with short actin filaments could therefore form a filamentous network comparable to the membrane cytoskeleton in red blood cells formed by spectrin and very short actin filaments (63), that spans the entire damaged area until other proteins such as XIRPs, α-actinin and globular actin are recruited and detectable actin filaments are assembled. For a model see Supplementary Material, Figure S2.

High-intensity exercise during muscle contraction leads to small injuries. To ensure continued striated, and especially, cardiac muscle function, fast and effective repair mechanisms are of vital importance. Indeed, we found multiple lesions not only in our cultured mouse cardiomyocytes, but also in hypertrophic hearts especially after aortic banding (our unpublished observations) that were highly similar to those found in skeletal muscle cells (1,2). Rapid protein relocalization therefore provides an essential mechanism during initial stages of repair, when it is important to stabilize damaged regions and avoid affection of neighboring sarcomeres. We show here that damaged cardiac myofibrils can be repaired in the contracting cell within only four hours. Furthermore, we examined the chronological sequence of myofibrillar repair in primary neonatal mouse cardiomyocytes and identified FLNc and aciculin as proteins involved in its earliest stages. Notably, at least in our model system, myofibrillar repair does not depend on *de novo* protein synthesis. Even though the expression level of certain mRNAs is known to rise enormously upon eccentric contractions (42,45), it takes at least 15 min until higher molecular mass proteins are synthesized in significant amounts. This highlights the importance of the properties of FLNc being a highly mobile protein that can rapidly relocalize to damaged areas in order to avoid collapse of myofibrils and to initiate their regeneration. In this respect it is interesting to note that in MFM-filaminopathy patients, in an MFM-filaminopathy knock-in mouse model, and in FLNcb mutant zebrafish that we recently characterized, the presence of large quantities of mutant FLNc, and/or the lack of sufficient levels of normal FLNc protein, leads to instability of myofibrils that is aggravated by exercise (23,34). We suggest that myofibril repair mimics, on a smaller scale, the process of myofibril assembly in nascent myofibrils and premyofibrils. The colocalization of FLNc, aciculin, Xin and XIRP2 in these structures and at the ends of myofibrils in myotendinous junctions and intercalated discs, where sarcomeres are added to existing myofibrils, further supports a cooperative role for these proteins during early stages of myofibril assembly.

Materials and Methods

Design of cDNA constructs

Construction of full length FLNc in pEGFP-N3 (Clontech) has been described before in (27). FLNc in pEGFP-N3-CAG was constructed by substitution of the CMV promoter by the CAG

promoter (CMV early enhancer, chicken β-actin promoter and the rabbit β-globin intron) (64). Full length α-actinin2 cDNA was amplified from a human heart cDNA library and cloned in pEGFP-N3-CAG and pRFP-N3-CAG, a pEGFP-N3-CAG vector in which EGFP was replaced by mRFP1 (mRFP1 cDNA was a kind gift from R. Campbell, La Jolla, CA). Full length XinA cDNA was excised from the pMypG vector (33) and cloned in pEGFP-N3-CAG. Lifeact-Ruby (65) was a kind gift from T. Quast, Bonn, Germany. Aciculin cDNA was excised from the pET23aT7 vector (2) and cloned in pRFP-N3, a pEGFP-N3 vector in which EGFP was replaced by mRFP1.

Mouse strains

Mice deficient for all isoforms of Xin (XinABC$^{-/-}$, Xirp1^{tm1Dofn}) were described before (66). To obtain mice deficient for Xin and XIRP2, mice from this strain were mated with homozygous XIRP2 hypomorphic mice (Xirp2^{tm1Itl}, 67). The obtained double homozygous mice completely lack all Xin isoforms and do not express detectable levels of XIRP2 protein.

Isolation and transfection of neonatal mouse cardiomyocytes

Hearts of 10 neonatal mice (P1) were dissected and pooled. Hearts were cut into small pieces, washed with phosphate-buffered saline (PBS) and incubated in dissociating enzyme solution (1 mg/ml collagenase B; Roche, Mannheim), 10 mM $CaCl_2$, 120 mM NaCl, 5.4 mM KCl, 5 mM $MgSO_4$, 5 mM sodium pyruvate, 20 mM taurine, 10 mM HEPES, 20 mM glucose, pH 6.9) for 15 min at 37 °C and 800 rpm in a thermomixer (HLC Biotech, Bovenden, Germany). Supernatants were removed and centrifuged for 3 min at 1000*g*. Cell pellets were resuspended in medium [20% FCS (Sigma-Aldrich), 2 mM NEAA, 100 U/ml penicillin, 100 μg/ml streptomycin, 50 pM β-mercaptoethanol in Iscove's modified Dulbecco's medium (IMDM; Gibco)] and sieved through a 100 μm pore nylon mesh of a cell strainer (BD Falcon). The procedure was repeated four times. All fractions were pooled and cells were pre-plated on uncoated cell culture dishes for 1–2 h until proceeding with transient transfections. Culture was maintained at 37 °C and 5% CO_2 in a humidified incubator.

After pre-plating, 10^6 non-attached cardiomyocytes were transfected using the Nucleofector technology as suggested by the manufacturer using program B-002 (Amaxa Rat Cardiomyocyte—Neonatal Nucleofector Kit, Lonza). After adding 500 μl medium, cells were immediately plated onto 0.1% gelatin-coated plastic dishes (ibidi).

Zebrafish maintenance and generation of transgenic strain

Zebrafish (*Danio rerio*) were maintained as previously described (68). The FLNc-EGFP expression vector was generated by subcloning full length human FLNc cDNA fused to EGFP from pEGFP-N3 into the multiple cloning site of the gateway destination vector (69) containing the skeletal muscle α-actin (*acta1*) promoter (70). The construct was injected, at 25 ng/μl, into one cell stage of Tu wild-type embryos along with 25 ng/μl codon optimized tol2 transposase mRNA, which was synthesized using the mMessage machine kit (Ambion) as per manufacturers protocol. Injected embryos were raised to adulthood and outcrossed to wild-type fish to identify transgenic founders.

FRAP and data analysis

FRAP experiments were performed with a Cell Observer SD Spinning Disk Confocal Microscope (Carl Zeiss, Jena, Germany) equipped with an external 473 nm laser coupled via a scanner (UGA-40, Rapp OptoElectronic, Hamburg) allowing bleaching of precisely defined ROI, using a Plan-Apochromat 63×/1.4 oil objective. Cardiomyocytes were permanently kept at 37 °C and 5% CO_2. Image processing was carried out using Zen2012 software (Carl Zeiss). For FRAP analyses three to seven independent experiments were performed and for each cell 1-3 ROIs were chosen for bleaching with areas of bleaching limited to one sarcomere or premyofibril. Photobleaching was done with 100% intensity of 473-nm laser (100 mW) for a pulse time of 1 ms with eight iterations. Images were taken before and immediately after bleaching. The fluorescence recovery was monitored for 200 s up to 30 min with an interval time of 0.1–10 s depending on the protein bleached. The ImageJ package Fiji (71) was used to determine fluorescence intensity of bleached and unbleached areas at each time point. Normalized FRAP curves were generated from raw data as previously described (72). FRAP data are displayed as mean of three to seven individual experiments. To generate corrected FRAP curves, the intensity in the bleached ROI ($I_{ROI}(t)$) and in the whole cell excluding the bleached area ($I_{whole}(t)$) at each time point were initially subtracted by the corresponding background intensity ($I_{bg}(t)$) and the fraction formed.

$$I_{cor}(t) = \frac{I_{ROI}(t) - I_{bg}(t)}{I_{whole}(t) - I_{bg}(t)}$$

Subsequently, normalization to the pre-bleach intensity was performed according to the following equitation:

$$I_{norm}(t) = \frac{I_{cor}(t) - I_{0\ cor}}{I_{pre\ cor} - I_{0\ cor}}$$

where $I_{norm}(t)$ is the normalized and corrected intensity, $I_{pre\ cor}$ the corrected intensity before photobleaching and $I_{0\ cor}$ the corrected first data point after photobleaching. Normalized fluorescence intensity versus time was plotted using Prism 4.0 (GraphPad Software). All results are expressed as mean ± SD.

Zebrafish FRAP experiments

Five day old FLNc-EGFP transgenic embryos were anesthetized with 0.16% Tricaine methanesulfonate in E3 embryo medium (5 mM NaCl, 0.17 mM KCl, 0.33 mM $CaCl_2$, 0.33 mM $MgSO_4$ in H_2O) and laterally mounted in 1% low melting agarose for FRAP experiments. For the cardiac experiments the heart rate was stopped by inclusion of 2,3-butanedione monoxime at 25 mM in the E3 media. Using a 20× 1.0 numerical aperture water dipping objective and a 488 nm laser on an LSM 710 confocal microscope (Carl Zeiss), a precise region of either cardiac or skeletal muscle was bleached with four iterations of 100% laser power (100 mW) and imaged every 0.5 s for 300 s. Imaging parameters were optimized for each sample to fully utilize the dynamic range of the detector. Fiji (71) was used to obtain fluorescence intensities in bleached and unbleached regions. Data analysis was performed as described (73) with the exception of the background correction, as all surrounding cells were fluorescent. Briefly, at each time point a ratio of bleached to unbleached intensities was

calculated ($I_{ratio}(t)$). To correct for any possible differences in intensities between bleached and unbleached regions, the $I_{ratio}(t)$ at each time point was divided by I_{mean}(pre), which is an average of *Iratio* at the four time points prior to photobleaching:

$$I_{cor}(t) = \frac{I_{ratio}(t)}{I_{mean}\ (pre)}$$

Subsequent normalization to obtain the $I_{norm}(t)$ was performed according to the cell culture FRAP studies:

$$I_{norm}(t) = \frac{I_{cor}(t) - I_{cor\ (0)}}{1 - I_{cor\ (0)}}$$

where $I_{norm}(t)$ is the normalized and corrected intensity, and $I_{cor\ (0)}$ the corrected first data point after photobleaching. Graphpad Prism was used to perform a two phase non linear regression analysis on each dataset to determine the slow and fast half-lives, and the mobile fraction, all of which are presented as mean ± SD. Data sets with ambiguous fits were omitted from further analysis.

Laser induced microdamage

Laser induced microdamage was performed using a confocal laser-scanning microscope equipped with a CO_2 chamber (LSM 710; Carl Zeiss). Transfected cardiomyocytes were kept at 37 °C and 5% CO_2 during the whole time lapse. Image processing was carried out using Zen2010 software (Carl Zeiss). For damage experiments a Plan-Apochromat 63×/1.4 oil differential interference contrast objective was used. ROIs were defined and irradiated with 100% intensity (30 mW) of a 405 nm laser beam one to four times until Z-disc splitting indicating myofibrillar damage occurred. It must be noted that in some experiments Z-disc splitting occured before complete bleaching of one or both fluorescent proteins (see e.g. aciculin-RFP in Fig. 4D). In these cases excessive irradiation was avoided to prevent irreversible damage. Images were taken every second for the first minute and subsequently every minute. For immunostaining cells were fixed with 4% paraformaldehyde and permeabilized with 0.5% Triton X-100 both in PBS. Cells were stained with anti-desmin antibody (clone D33; Dakopatts, Glostrup, Denmark) followed by Cy5-conjugated goat anti-mouse IgG secondary antibody (Jackson Immunoresearch, Suffolk, UK), and coumarin-conjugated phalloidin (Sigma).

In some experiments protein synthesis was inhibited by addition of 50 μM cycloheximide (Sigma-Aldrich) to the culture media 1 h before starting the experiments. Cells were kept in this medium during the entire analysis.

Supplementary Material

Supplementary Material is available at *HMG* online.

Acknowledgements

We thank Dr T. Quast, Bonn, Germany and R. Campbell, La Jolla, CA, USA for donating the Lifeact-Ruby construct and the mRFP1 cDNA, respectively, and Mrs. B. Bockmühl, N. Thum-Schmitz, Y. Matuschek and N. Euler for excellent technical assistance.

Conflict of Interest statement. None declared.

Funding

This work was supported by the German Research foundation (FOR1228 and FOR1352 to D.O.F.) and the Seventh Framework Programme for Research and Technological Development of the EU (MUZIC; D.O.F.). The zebrafish work was supported by an NHMRC discovery project grant (no. 1010110). The contents of this manuscript are solely the responsibility of the authors and do not reflect the views of NHMRC.

References

1. Eulitz, S., Sauer, F., Pelissier, M.C., Boisguerin, P., Molt, S., Schuld, J., Orfanos, Z., Kley, R.A., Volkmer, R., Wilmanns, M. *et al.* (2013) Identification of Xin-repeat proteins as novel ligands of the SH3 domains of nebulin and nebulette and analysis of their interaction during myofibril formation and remodeling. *Mol. Biol. Cell*, **24**, 3215–3226.
2. Molt, S., Bührdel, J.B., Yakovlev, S., Schein, P., Orfanos, Z., Kirfel, G., Winter, L., Wiche, G., Van der Ven, P.F.M., Rottbauer, W. *et al.* (2014) Aciculin interacts with filamin C and Xin and is essential for myofibril assembly, remodeling and maintenance. *J. Cell Sci.*, **127**, 3578–3592.
3. Nilsson, M.I., Nissar, A.A., Al-Sajee, D., Tarnopolsky, M.A., Parise, G., Lach, B., Fürst, D.O., Van der Ven, P.F.M., Kley, R.A. and Hawke, T.J. (2013) Xin is a marker of skeletal muscle damage severity in myopathies. *Am. J. Pathol.*, **183**, 1703–1709.
4. Orfanos, Z., Gödderz, M.P.O., Soroka, E., Gödderz, T., Rumyantseva, A., Van der Ven, P.F.M., Hawke, T.J. and Fürst, D.O. (2016) Breaking sarcomeres by in vitro exercise. *Sci. Rep.*, **6**, 19614.
5. Nakamura, F., Stossel, T.P. and Hartwig, J.H. (2011) The filamins: organizers of cell structure and function. *Cell Adh. Migr.*, **5**, 160–169.
6. Van der Flier, A. and Sonnenberg, A. (2001) Structural and functional aspects of filamins. *Biochim. Biophys. Acta*, **1538**, 99–117.
7. Zhou, X., Boren, J. and Akyurek, L.M. (2007) Filamins in cardiovascular development. *Trends Cardiovasc. Med.*, **17**, 222–229.
8. Stossel, T.P., Condeelis, J., Cooley, L., Hartwig, J.H., Noegel, A., Schleicher, M. and Shapiro, S.S. (2001) Filamins as integrators of cell mechanics and signalling. *Nat. Rev. Mol. Cell Biol.*, **2**, 138–145.
9. Feng, Y. and Walsh, C.A. (2004) The many faces of filamin: a versatile molecular scaffold for cell motility and signalling. *Nat. Cell Biol.*, **6**, 1034–1038.
10. Daniel, P.B., Morgan, T., Alanay, Y., Bijlsma, E., Cho, T.J., Cole, T., Collins, F., David, A., Devriendt, K., Faivre, L. *et al.* (2012) Disease-associated mutations in the actin-binding domain of filamin B cause cytoplasmic focal accumulations correlating with disease severity. *Hum. Mutat.*, **33**, 665–673.
11. Fürst, D.O., Goldfarb, L.G., Kley, R.A., Vorgerd, M., Olivé, M. and Van der Ven, P.F.M. (2013) Filamin C-related myopathies: pathology and mechanisms. *Acta Neuropathol.*, **125**, 33–46.
12. Chiang, W., Greaser, M.L. and Lyons, G.E. (2000) Filamin isogene expression during mouse myogenesis. *Dev. Dyn.*, **217**, 99–108.
13. Thompson, T.G., Chan, Y.M., Hack, A.A., Brosius, M., Rajala, M., Lidov, H.G., McNally, E.M., Watkins, S. and Kunkel, L.M.

(2000) Filamin 2 (FLN2). A muscle-specific sarcoglycan interacting protein. *J. Cell Biol.*, **148**, 115–126.
14. Xie, Z., Xu, W., Davie, E.W. and Chung, D.W. (1998) Molecular cloning of human ABPL, an actin-binding protein homologue. *Biochem. Biophys. Res. Commun.*, **251**, 914–919.
15. Van der Ven, P.F.M., Obermann, W.M.J., Lemke, B., Gautel, M., Weber, K. and Fürst, D.O. (2000) Characterization of muscle filamin isoforms suggests a possible role of γ-filamin/ABP-L in sarcomeric Z-disc formation. *Cell Motil. Cytoskeleton*, **45**, 149–162.
16. Faulkner, G., Pallavicini, A., Comelli, A., Salamon, M., Bortoletto, G., Ievolella, C., Trevisan, S., Kojic, S., Dalla, V.F., Laveder, P. *et al.* (2000) FATZ: a filamin-, actinin-, and telethonin-binding protein of the Z-disk of skeletal muscle. *J. Biol. Chem.*, **275**, 41234–41242.
17. Frey, N. and Olson, E.N. (2002) Calsarcin-3, a novel skeletal muscle-specific member of the calsarcin family, interacts with multiple Z-disc proteins. *J. Biol. Chem.*, **277**, 13998–14004.
18. Takada, F., Vander Woude, D.L., Tong, H.Q., Thompson, T.G., Watkins, S.C., Kunkel, L.M. and Beggs, A.H. (2001) Myozenin: an α-actinin- and γ-filamin-binding protein of skeletal muscle Z lines. *Proc. Natl. Acad. Sci. USA*, **98**, 1595–1600.
19. Van der Ven, P.F.M., Wiesner, S., Salmikangas, P., Auerbach, D., Himmel, M., Kempa, S., Hayeß, K., Pacholsky, D., Taivainen, A., Schröder, R. *et al.* (2000) Indications for a novel muscular dystrophy pathway. γ-filamin, the muscle-specific filamin isoform, interacts with myotilin. *J. Cell Biol.*, **151**, 235–248.
20. Linnemann, A., Van der Ven, P.F.M., Vakeel, P., Albinus, B., Simonis, D., Bendas, G., Schenk, J.A., Micheel, B., Kley, R.A. and Fürst, D.O. (2010) The sarcomeric Z-disc component myopodin is a multiadapter protein that interacts with filamin and α-actinin. *Eur. J. Cell Biol.*, **89**, 681–692.
21. Zhang, M., Liu, J., Cheng, A., Deyoung, S.M. and Saltiel, A.R. (2007) Identification of CAP as a costameric protein that interacts with filamin C. *Mol. Biol. Cell*, **18**, 4731–4740.
22. Dalkilic, I., Schienda, J., Thompson, T.G. and Kunkel, L.M. (2006) Loss of FilaminC (FLNc) results in severe defects in myogenesis and myotube structure. *Mol. Cell. Biol.*, **26**, 6522–6534.
23. Ruparelia, A.A., Zhao, M., Currie, P.D. and Bryson-Richardson, R.J. (2012) Characterization and investigation of zebrafish models of filamin-related myofibrillar myopathy. *Hum. Mol. Genet.*, **21**, 4073–4083.
24. Bönnemann, C.G., Thompson, T.G., Van der Ven, P.F.M., Goebel, H.H., Warlo, I., Vollmers, B., Reimann, J., Herms, J., Gautel, M., Takada, F. *et al.* (2003) Filamin C accumulation is a strong but nonspecific immunohistochemical marker of core formation in muscle. *J. Neurol. Sci.*, **206**, 71–78.
25. Sewry, C.A. (2000) Immunocytochemical analysis of human muscular dystrophy. *Microsc. Res. Tech.*, **48**, 142–154.
26. Claeys, K.G., Van der Ven, P.F.M., Behin, A., Stojkovic, T., Eymard, B., Dubourg, O., Laforet, P., Faulkner, G., Richard, P., Vicart, P. *et al.* (2009) Differential involvement of sarcomeric proteins in myofibrillar myopathies: a morphological and immunohistochemical study. *Acta Neuropathol.*, **117**, 293–307.
27. Duff, R.M., Tay, V., Hackman, P., Ravenscroft, G., McLean, C., Kennedy, P., Steinbach, A., Schöffler, W., Van der Ven, P.F.M., Fürst, D.O. *et al.* (2011) Mutations in the N-terminal actin-binding domain of filamin C cause a distal myopathy. *Am. J. Hum. Genet.*, **88**, 729–740.
28. Vorgerd, M., Van der Ven, P.F.M., Bruchertseifer, V., Löwe, T., Kley, R.A., Schröder, R., Lochmüller, H., Himmel, M., Koehler, K., Fürst, D.O. *et al.* (2005) A mutation in the dimerization domain of filamin c causes a novel type of autosomal dominant myofibrillar myopathy. *Am. J. Hum. Genet.*, **77**, 297–304.
29. Guergueltcheva, V., Peeters, K., Baets, J., Ceuterick-de Groote, C., Martin, J.J., Suls, A., Vriendt, E., de, Mihaylova, V., Chamova, T. *et al.* (2011) Distal myopathy with upper limb predominance caused by filamin C haploinsufficiency. *Neurology*, **77**, 2105–2114.
30. Brodehl, A., Ferrier, R.A., Hamilton, S.J., Greenway, S.C., Brundler, M.A., Yu, W., Gibson, W.T., McKinnon, M.L., McGillivray, B., Alvarez, N. *et al.* (2015) Mutations in *FLNC* are associated with familial restrictive cardiomyopathy. *Hum. Mutat.*, **37**, 269–279.
31. Valdés-Mas, R., Gutiérrez-Fernández, A., Gómez, J., Coto, E., Astudillo, A., Puente, D.A., Reguero, J.R., Alvarez, V., Morís, C., León, D. *et al.* (2014) Mutations in filamin C cause a new form of familial hypertrophic cardiomyopathy. *Nat. Commun.*, **5**, 5326.
32. Kley, R.A., Maerkens, A., Leber, Y., Theis, V., Schreiner, A., Van der Ven, P.F.M., Uszkoreit, J., Stephan, C., Eulitz, S., Euler, N. *et al.* (2013) A combined laser microdissection and mass spectrometry approach reveals new disease relevant proteins accumulating in aggregates of filaminopathy patients. *Mol. Cell. Proteomics*, **12**, 215–227.
33. Van der Ven, P.F.M., Ehler, E., Vakeel, P., Eulitz, S., Schenk, J.A., Milting, H., Micheel, B. and Fürst, D.O. (2006) Unusual splicing events result in distinct Xin isoforms that associate differentially with filamin C and Mena/VASP. *Exp. Cell Res.*, **312**, 2154–2167.
34. Chevessier, F., Schuld, J., Orfanos, Z., Plank, A.C., Wolf, L., Maerkens, A., Unger, A., Schlötzer-Schrehardt, U., Kley, R.A., von Hörsten, S. *et al.* (2015) Myofibrillar instability exacerbated by acute exercise in filaminopathy. *Hum. Mol. Genet.*, **24**, 7207–7220.
35. Yu, J.G., Fürst, D.O. and Thornell, L.E. (2003) The mode of myofibril remodelling in human skeletal muscle affected by DOMS induced by eccentric contractions. *Histochem. Cell Biol.*, **119**, 383–393.
36. Yu, J.G., Carlsson, L. and Thornell, L.E. (2004) Evidence for myofibril remodeling as opposed to myofibril damage in human muscles with DOMS: an ultrastructural and immunoelectron microscopic study. *Histochem. Cell Biol.*, **121**, 219–227.
37. Carlsson, L., Yu, J.G., Moza, M., Carpén, O. and Thornell, L.E. (2007) Myotilin – a prominent marker of myofibrillar remodelling. *Neuromusc. Disord.*, **17**, 61–68.
38. Carlsson, L., Yu, J.G. and Thornell, L.E. (2008) New aspects of obscurin in human striated muscles. *Histochem. Cell Biol.*, **130**, 91–103.
39. Van der Flier, A., Kuikman, I., Kramer, D., Geerts, D., Kreft, M., Takafuta, T., Shapiro, S.S. and Sonnenberg, A. (2002) Different splice variants of filamin-B affect myogenesis, subcellular distribution, and determine binding to integrin β subunits. *J. Cell Biol.*, **156**, 361–376.
40. Soumpasis, D.M. (1983) Theoretical analysis of fluorescence photobleaching recovery experiments. *Biophys. J.*, **41**, 95–97.
41. Braeckmans, K., Peeters, L., Sanders, N.N., de Smedt, S.C. and Demeester, J. (2003) Three-dimensional fluorescence recovery after photobleaching with the confocal scanning laser microscope. *Biophys. J.*, **85**, 2240–2252.,
42. Barash, I.A., Mathew, L., Ryan, A.F., Chen, J. and Lieber, R.L. (2004) Rapid muscle-specific gene expression changes after

a single bout of eccentric contractions in the mouse. *Am. J. Physiol. Cell Physiol.*, **286**, C355–C364.
43. Hawke, T.J., Atkinson, D.J., Kanatous, S.B., Van der Ven, P.F.M., Goetsch, S.C. and Garry, D.J. (2007) Xin, an actin binding protein, is expressed within muscle satellite cells and newly regenerated skeletal muscle fibers. *Am. J. Physiol. Cell Physiol.*, **293**, C1636–C1644.
44. Kley, R.A., Hellenbroich, Y., Van der Ven, P.F.M., Fürst, D.O., Huebner, A., Bruchertseifer, V., Peters, S.A., Heyer, C.M., Kirschner, J., Schröder, R. *et al.* (2007) Clinical and morphological phenotype of the filamin myopathy: a study of 31 German patients. *Brain*, **130**, 3250–3264.
45. MacNeil, L.G., Melov, S., Hubbard, A.E., Baker, S.K. and Tarnopolsky, M.A. (2010) Eccentric exercise activates novel transcriptional regulation of hypertrophic signaling pathways not affected by hormone changes. *PLoS One*, **5**, e10695.
46. Wang, J., Shaner, N., Mittal, B., Zhou, Q., Chen, J., Sanger, J.M. and Sanger, J.W. (2005) Dynamics of Z-band based proteins in developing skeletal muscle cells. *Cell Motil. Cytoskeleton*, **61**, 34–48.
47. Sanger, J.W., Wang, J., Fan, Y., White, J. and Sanger, J.M. (2010) Assembly and dynamics of myofibrils. *J. Biomed. Biotechnol.*, **2010**, 858606.
48. Wang, J., Dube, D.K., Mittal, B., Sanger, J.M. and Sanger, J.W. (2011) Myotilin dynamics in cardiac and skeletal muscle cells. *Cytoskeleton*, **68**, 661–670.
49. Frank, D. and Frey, N. (2011) Cardiac Z-disc signaling network. *J. Biol. Chem.*, **286**, 9897–9904.
50. Arndt, V., Dick, N., Tawo, R., Dreiseidler, M., Wenzel, D., Hesse, M., Fürst, D.O., Saftig, P., Saint, R., Fleischmann, B.K. *et al.* (2010) Chaperone-assisted selective autophagy is essential for muscle maintenance. *Curr. Biol.*, **20**, 143–148.
51. Ulbricht, A., Eppler, F.J., Tapia, V.E., Van der Ven, P.F.M., Hampe, N., Hersch, N., Vakeel, P., Stadel, D., Haas, A., Saftig, P. *et al.* (2013) Cellular mechanotransduction relies on tension-induced and chaperone-assisted autophagy. *Curr. Biol.*, **23**, 430–435.
52. Skwarek-Maruszewska, A., Hotulainen, P., Mattila, P.K. and Lappalainen, P. (2009) Contractility-dependent actin dynamics in cardiomyocyte sarcomeres. *J. Cell Sci.*, **122**, 2119–2126.
53. Hartman, T.J., Martin, J.L., Solaro, R.J., Samarel, A.M. and Russell, B. (2009) CapZ dynamics are altered by endothelin-1 and phenylephrine via PIP2- and PKC-dependent mechanisms. *Am. J. Physiol. Cell Physiol.*, **296**, C1034–C1039.
54. Ruparelia, A.A., Oorschot, V., Ramm, G. and Bryson-Richardson, R.J. (2016) FLNC myofibrillar myopathy results from impaired autophagy and protein insufficiency. *Hum. Mol. Genet.*, pii: ddw080.
55. Löwe, T., Kley, R.A., Van der Ven, P.F.M., Himmel, M., Huebner, A., Vorgerd, M. and Fürst, D.O. (2007) The pathomechanism of filaminopathy: altered biochemical properties explain the cellular phenotype of a protein aggregation myopathy. *Hum. Mol. Genet.*, **16**, 1351–1358.
56. Chang, Y.W., Chang, Y.T., Wang, Q., Lin, J.J., Chen, Y.J. and Chen, C.C. (2013) Quantitative phosphoproteomic study of pressure-overloaded mouse heart reveals dynamin-related protein 1 as a modulator of cardiac hypertrophy. *Mol. Cell. Proteomics*, **12**, 3094–3107.
57. Murray, J.T., Campbell, D.G., Peggie, M., Alfonso, M. and Cohen, P. (2004) Identification of filamin C as a new physiological substrate of PKBα using KESTREL. *Biochem. J.*, **384**, 489–494.
58. Sequea, D.A., Sharma, N., Arias, E.B. and Cartee, G.D. (2013) Greater filamin C, GSK3alpha, and GSK3beta serine phosphorylation in insulin-stimulated isolated skeletal muscles of calorie restricted 24 month-old rats. *Mech. Ageing Dev.*, **134**, 60–63.
59. Otten, C., Van der Ven, P.F.M., Lewrenz, I., Paul, S., Steinhagen, A., Busch-Nentwich, E., Eichhorst, J., Wiesner, B., Stemple, D., Strähle, U. *et al.* (2012) Xirp proteins mark injured skeletal muscle in zebrafish. *PLoS One*, **7**, e31041.
60. Yu, J.G. and Russell, B. (2005) Cardiomyocyte remodeling and sarcomere addition after uniaxial static strain in vitro. *J. Histochem. Cytochem.*, **53**, 839–844.
61. Ehrlicher, A.J., Nakamura, F., Hartwig, J.H., Weitz, D.A. and Stossel, T.P. (2011) Mechanical strain in actin networks regulates FilGAP and integrin binding to filamin A. *Nature*, **478**, 260–263.
62. Rognoni, L., Stigler, J., Pelz, B., Ylänne, J. and Rief, M. (2012) Dynamic force sensing of filamin revealed in single-molecule experiments. *Proc. Natl. Acad. Sci. USA*, **109**, 19679–19684.
63. Fowler, V.M. (1996) Regulation of actin filament length in erythrocytes and striated muscle. *Curr. Opin. Cell Biol.*, **8**, 86–96.
64. Miyazaki, J., Takaki, S., Araki, K., Tashiro, F., Tominaga, A., Takatsu, K. and Yamamura, K. (1989) Expression vector system based on the chicken beta-actin promoter directs efficient production of interleukin-5. *Gene*, **79**, 269–277.
65. Riedl, J., Crevenna, A.H., Kessenbrock, K., Yu, J.H., Neukirchen, D., Bista, M., Bradke, F., Jenne, D., Holak, T.A., Werb, Z. *et al.* (2008) Lifeact: a versatile marker to visualize F-actin. *Nat. Methods*, **5**, 605–607.
66. Otten, J., Van der Ven, P.F.M., Vakeel, P., Eulitz, S., Kirfel, G., Brandau, O., Boesl, M., Schrickel, J.W., Linhart, M., Hayeß, K. *et al.* (2010) Complete loss of murine Xin results in a mild cardiac phenotype with altered distribution of intercalated discs. *Cardiovasc. Res.*, **85**, 739–750.
67. McCalmon, S.A., Desjardins, D.M., Ahmad, S., Davidoff, K.S., Snyder, C.M., Sato, K., Ohashi, K., Kielbasa, O.M., Mathew, M., Ewen, E.P. *et al.* (2010) Modulation of angiotensin II-mediated cardiac remodeling by the MEF2A target gene Xirp2. *Circ. Res.*, **106**, 952–960.
68. Westerfield, M. (1993) *The Zebrafish Book*. University of Oregon Press, Eugene, OR.
69. Kwan, K.M., Fujimoto, E., Grabher, C., Mangum, B.D., Hardy, M.E., Campbell, D.S., Parant, J.M., Yost, H.J., Kanki, J.P. and Chien, C.B. (2007) The Tol2kit: a multisite gateway-based construction kit for Tol2 transposon transgenesis constructs. *Dev. Dyn.*, **236**, 3088–3099.
70. Higashijima, S., Okamoto, H., Ueno, N., Hotta, Y. and Eguchi, G. (1997) High-frequency generation of transgenic zebrafish which reliably express GFP in whole muscles or the whole body by using promoters of zebrafish origin. *Dev. Biol.*, **192**, 289–299.
71. Schindelin, J., Arganda-Carreras, I., Frise, E., Kaynig, V., Longair, M., Pietzsch, T., Preibisch, S., Rueden, C., Saalfeld, S., Schmid, B. *et al.* (2012) Fiji: an open-source platform for biological-image analysis. *Nat. Methods*, **9**, 676–682.
72. Al Tanoury, Z., Schaffner-Reckinger, E., Halavatyi, A., Hoffmann, C., Moes, M., Hadzic, E., Catillon, M., Yatskou, M. and Friederich, E. (2010) Quantitative kinetic study of the actin-bundling protein L-plastin and of its impact on actin turn-over. *PLoS One*, **5**, e9210.
73. Sanger, J.W., Wang, J., Holloway, B., Du, A. and Sanger, J.M. (2009) Myofibrillogenesis in skeletal muscle cells in zebrafish. *Cell Motil. Cytoskeleton*, **66**, 556–566.